SPACE-BORNE CLOUD-NATIVE SATELLITE-DERIVED BATHYMETRY (SDB) MODELS USING ICESat-2 and SENTINEL-2

N. Thomas[1,2], A. P. Pertiwi[3], D. Traganos[3], D. Lagomasino[4], D. Poursanidis[5], S. Moreno[4] and L. Fatoyinbo[2]

[1]Earth System Science Interdisciplinary Center (ESSIC), University of Maryland, College Park, MD USA

[2]Biospheric Sciences Laboratory, NASA Goddard Space Flight Center, Greenbelt, MD USA

[3]German Aerospace Center (DLR), Remote Sensing Technology Institute - Rutherfordstrasse 2, 12489 Berlin, Germany

[4]Department of Coastal Studies, East Carolina University, Wanchese, NC, USA

[5]Foundation for Research and Technology - Hellas (FORTH), Institute of Applied and Computational Mathematics, N. Plastira 100, Vassilika Vouton, 70013 Heraklion, Greece

Corresponding author: Nathan Thomas (nathan.m.thomas@nasa.gov), Avi Putri Pertiwi (avi.pertiwi@dlr.de)

Key Points:

- Nearshore bathymetric depths can be retrieved using ICESat-2 lidar data
- ICESat-2 bathymetric data can train Sentinel-2 Satellite Derived Bathymetry (SDB) models at shoreline to national scales
- The fusion of ICESat-2 and Sentinel-2 data in the cloud paves the way for accurate nearshore bathymetry mapping from space

Abstract

Shallow nearshore coastal waters provide a wealth of societal, economic and ecosystem services, yet their topographic structure is poorly mapped due to a reliance upon expensive and time intensive methods. Space-borne bathymetric mapping has helped address these issues, but has remained dependent upon *in situ* measurements. Here we fuse ICESat-2 lidar data with Sentinel-2 optical imagery, within the Google Earth Engine geospatial cloud platform, to create wall-to-wall high-resolution bathymetric maps at regional-to-national scales in Florida, Crete and Bermuda. ICESat-2 bathymetric classified photons are used to train three Satellite Derived Bathymetry (SDB) methods, including Lyzenga, Stumpf and Support Vector Regression algorithms. For each study site the Lyzenga algorithm yielded the lowest RMSE (approx. 10-15%) when compared with *in situ* NOAA DEM data. We demonstrate a means of using ICESat-2 for both model calibration and validation, thus cementing a pathway for fully space-borne estimates of nearshore bathymetry in shallow, clear water environments.

Plain Language Summary

Knowledge of the depth of the shallow seafloor in coastal waters is needed for a wide range of applications, including navigation and habitat monitoring. Mapping water depth in these locations is expensive, arduous and sometimes dangerous. To overcome some of these challenges, we used multiple satellite datasets to map water depth in several unique coastal environments. ICESat-2 lidar data is able to sample the depth of the seabed along straight lines in clear water and is then combined with other satellite imagery to derive wall-to-wall water depth maps using well known regression algorithms. The results of these models are accurate maps of water depth from space, containing a level of detail that can exceed some field collected measurements.

1 Introduction

Accurate and current bathymetric maps are essential for informing coastal management decision making. Emerging demands of the blue economy will open up new opportunities, but could also have significant impacts on coastal regions and coastal habitats around the world (LiVecci et al, 2019). Several key markets that will demand resources from the nearshore environment have been identified for future and continued development including, marine navigation, aquaculture, coastal resilience and disaster recovery, and isolated power supply. Technological innovation that allows for contemporary nearshore and seafloor maps with regular repeat observations will enable proper Marine Spatial Planning (MSP) and sharing of coastal waters (Lester et al, 2018; Foley et al, 2010).

Competing sectors of the Blue Economy will change the bathymetry of nearshore waterways and coastal regions in a variety of ways. Continued and new dredging to meet shipping and navigation demands will increase channel depth and quantity of material spoil (Bishop et al, 2006). Similarly, aquaculture practices such as kelp and oyster farming will reduce erosion and increase sediment accumulation (Zhang et al, 2020; de Paiva et al, 2018). These practices are predicted to change the structure of the seafloor which will have local-scale implications for sub-aquatic ecosystems and nearshore navigation, by causing rapid changes in benthic morphology. In addition, nearshore structure is increasingly being looked to as a source of nature-based risk reduction solutions, including the use of natural barriers to sea level rise and storm surges (Spalding et al, 2014). For improved coastal resilience assessments, accurate maps of the seafloor are a critical parameter in measuring the wave attenuation of benthic habitats, like seagrasses and coral reefs, (Narayan et al, 2016) and the erosion potentional of dune-lined beaches (Schweiger et al, 2020), but up-to-date and repeatable observations of sediment stability

(e.g. changes in water depth) and structural complexity are needed (Christianen et al, 2013: Harris et al, 2018). These and other processes are not fully captured by current, openly available coarse bathymetry data (Wolfl et al, 2019), which are limited in spatial and temporal resolution. Increasing the resolutions of bathymetric data requires financial investment and substantial energy expenditure to conduct more comprehensive or frequent surveys, particularly to capture the detail required in the nearshore coastal environment.

Globally, there are several initiatives that procure bathymetric data collected by hydrographic, oceanographic, and other vessels such as the International Hydrographic Organization Data Centre for Digital Bathymetry (IHO DCDB; Marks, 2019), European Marine Observation and Data Network (EMODnet; Emodnet, 2016), the Global Multi-Resolution Topography (GMRT; Ryan et al, 2009) synthesis and the General Bathymetric Chart of the Oceans (GEBCO; Kapoor, 1981). While these initiatives ensure that global bathymetric data are available at satisfactory resolutions across large expanses of open ocean, these data are not adequate for use in shallow waters where the vertical and spatial resolution is insufficient. With high-resolution elevation data available for land surfaces (e.g., TanDEM-X; Wessel et al, 2018), this leaves a corridor of missing data between the land and open ocean, where high quality data are most required. Singlebeam (SBES) and Multibeam Echo Sounders (MBES) are commonly deployed on small craft for local-scale high-resolution mapping (Janowski et al, 2018) but collecting such data in shallow water can be hazardous and time consuming. Bathymetric lidar data are well suited to fill this gap and can be acquired from airborne systems (Kim et al, 2017) to circumvent navigation in busy shipping traffic, however they are economically expensive and time-intensive to gather over large areas, particularly where frequent repeat surveys to capture rapid changes are required.

Recent advances in Satellite-Derived Bathymetry (SDB) using multispectral Earth Observations have lead to new methodological developments and applications through increased spatial resolution and improved estimations (Traganos et al, 2018a; Caballero et al, 2019; Caballero and Stumpf, 2020a, 2020b; Casal et al, 2019, 2020; Daly et al, 2020; Mateo-Perez et al. 2020). Commercial satellite imagery has also been used to improve modeling on shallow coastal bathymetry by achieving spatial resolutions of 3-m/pixel and daily revisits (Li et al, 2019; Poursanidis et al, 2019; Lyons et al, 2020). A number of SDB studies have improved water depth retrieval through empirical correlations of surface reflectance with field-acquired depth points (Lyzenga, 1978; Stumpf et al, 2003); machine learning that combines surface reflectance and in-situ data (Pan et al, 2015; Geyman and Maloof, 2019; Albright and Glennie, 2020); automatic tuning of SDB to water column conditions (Kerr and Purkis, 2018; Li et al, 2019); inverting wave celerity based on the temporal offset between the satellite's bands (Daly et al, 2020) and physics-based inversion algorithms that produce highly-accurate SDB estimations but at the expense of restricted scalability due to the required computational power for the inversion (Casal et al, 2020). Despite the advances in SDB and the recent increased availability of cloud-computing platforms such as the Google Earth Engine and Amazon Web Services, most approaches still rely on airborne/shipborne data and local computing resources.

An ability to widely collect consistent SDB calibration and validation data will alleviate some of the limitations in deriving routine nearshore bathymetry. The first release of ICESat-2 data highlighted the potential to acquire global bathymetric lidar data in shallow (<40m) coastal waters (Markus et al, 2017; Parrish et al, 2019). This exciting new capability is especially timely for coastal ecosystem studies as it paves the way for purely spaceborne SDB approaches in the optically shallow global seascape realm (Albright and Glennie, 2020, Ma et al. 2020). Such

fusion approaches between satellite-based multispectral imagery and lidar data are now feasible and could significantly reduce the needed time, costs, and computation to produce seamless SDB maps, especially in data poor regions.

In the present study, we have developed one of the first fully space-based approaches to measure nearshore bathymetry in optically shallow waters. The SDBs presented here are derived from a newly designed cloud-native workflow within the Google Earth Engine cloud platform (Gorelick et al, 2017) using multi-temporal Sentinel-2A/B data (Traganos et al, 2018a) and ICESat-2 lidar observations (Parrish et al, 2019). Our primary aim is to evaluate the accuracy, scalability and uncertainties of this approach for retrieving SDB, in comparison to freely availble bathymetric Digital Elevation Models (DEMs).

2 Materials and Methods

2.1 Data

2.1.1 ICESat-2

The Ice, Cloud and Elevation Satellite-2 (ICESat-2; IS-2) is a spaceborne altimeter launched in September 2018. IS-2 carries the Advanced Topographic Laser Altimeter System (ATLAS) which is a photon counting lidar, composed of three pairs of beams each separated by 3.3 km, with 90 m between each pair. The pairs of lasers are divided into a strong and a weak beam, based on a 1:4 energy ratio. Each laser has a repetition rate of 10 kHz with a wavelength of 532 nm. Each photon shot is separated by 70 cm with a footprint size of approximately13 m. IS-2 geolocated photon data is provided in the ATL03 product which is disseminated through the National Snow and Ice Data Center (NSIDC).

2.1.2 Sentinel-2

The estimation of satellite-derived bathymetry is based on Copernicus Sentinel-2 data and is performed end-to-end within the Google Earth Engine (GEE) geospatial computing platform. Sentinel-2 is a twin-satellite mission with 10-m spatial resolution and a 5-day revisit period and which have provided open and free data since June 2015. In this study, we utilized both Level-1C (L1C) top-of-atmosphere (TOA) reflectance (23 June 2015 - Present) and Level-2A (L2A) atmospherically corrected surface reflectance (SR) (28 March 2017 - Present) datasets, available within GEE.

2.1.3 Ancillary Bathymetric Data

2.1.3.1 NOAA Bathymetry

The Bermuda and Biscayne Bay, Florida topographic-bathymetric Digital Elevation models (DEMs) were acquired from the NOAA National Centers for Environmental Information using the Bathymetric Data Viewer portal (https://maps.ngdc.noaa.gov/viewers/bathymetry/). The Bermuda DEM, at a resolution of 1 to 3 arc-second spatial resolution, was collected by multiple institutions (e.g., Government of Bermuda, California State University, and NOAA) over a period of 20 (1993-2012; Sutherland et al, 2013). Data was derived from a variety of measurement techniques including topographic surveys, bathymetric lidar, gridded and raw multibeam bathymetry, and nautical chart sounding depth, all combined to create a 1 arc-second DEM. The Biscayne Bay (S200) DEM has a 1 arc-second spatial resolution which was derived from nearly 150,000 soundings collected within the bay from 12 different surveys over a period of 63 years (1930-1993; NOAA, 1998). The data was gridded by prioritizing more recent data and/or highest resolution data over older and lower resolution data. Where data coverage was sparse, generic interpolation and extrapolation models were used to fill gaps.

2.1.3.2 Singlebeam Sonar

Using low cost fishfinder tools, the collection of bathymetry data at the Gulf of Chania (Crete) was completed June - July 2020 based on the method of Poursanidis et al (2018), covering a depth range of 2 to 55 m.

2.2 Study Sites

2.2.1 Natura 2000 GR4340003, Crete

The Natura 2000 site GR4340003 is found on the North West of the the island of Crete, Greece. The Island bounds the southern border of the Aegean Sea, approximately 160 km south of the

Greek mainland, and has an area of 8,336 km^2 and a coastline of 1,046 km. Specifically, the Natura 2000 site GR4340003 “Chersonisos Rodopou – Paralia Maleme – Kolpos Chanion” includes Rodopos peninsula and the coastal area from Kolympari to Platanias, at the NW part of Crete, approximately 20 km from Chania city. The marine part of the site extends to a depth of 50 m and is characterized by the presence of *Posidonia oceanica* seagrass beds.

2.2.2 Biscayne Bay, Florida

Biscayne Bay is an estuary on the east coast of South Florida (USA) that is ecologically diverse and serves as a nursery for many marine species. The bay is heavily influenced by human activities such as boating, diving, recreational and commercial fishing, and serves as a major shipping port. Around the major shipping port and private docks there are incised channels that can exceed 15 m in depth and require regular dredging. The bay faces many ecological concerns mostly due to declining water quality and freshwater inflows caused by increased runoff (Carey et al, 2011). The benthic habitats of the central and southern regions of the bay are dominated by seagrass, which includes *Thalassia testudinum*, with sporadic patch reef complexes (Lirman et al, 2008).

2.2.3 Bermuda

Bermuda is a subtropical Caribbean Island over 1200 km north of the Bahamas, and 965 km east of North Carolina. It is surrounded by the northernmost coral reef assemblage in the Atlantic Ocean and also includes seagrass beds, mangroves, salt marshes, and rocky and sandy intertidal areas (Coates et al, 2013). The reef complex forms a 2 to 10 m deep, 1.5 km wide rim that surrounds the northern part of the islands. Patch reefs within the lagoon can be found within 1-2 m of the water surface. Marine transport is important to the island as most resources are imported

and shipping channels have been modified to accommodate large cruise ships. Channel dredging has led to water quality issues in nearby regions (Lester et al, 2016).

2.3 Satellite-Derived Bathymetry Modeling

2.3.1 ICESat-2 Bathymetric Photons

ICESat-2 ATL03 data was queried via the Open Altimetry online portal (https://www.openaltimetry.org) where it was subset and downloaded over our regions of interest from the NSIDC server in HDF5 format (Figure 1, a, b, c). The ATL03 product does not record the true location and elevation of sub-aquatic photons due to the refraction of the laser at the air/water interface and the delayed travel time of the laser through the water column. To correct the offset, accurate longitude, latitude, and photon height corrections were performed using the methods of Parrish et al. (2019). This uses the spacecraft geometry and incident laser refraction at the water surface to correct target photon depths, using inputs that include the IS-2 instrument wavelength (532 nm), water salinity (35 Practical Salinity Units (PSU)) at atmospheric pressure and location specific ocean temperatures. Photons were initially transformed to orthometric height (EGM2008), and local UTM zone. Water surface photons were then manually selected using an interactive python plot. The average of the selected water surface photons was defined as the water surface model, from which photons below this were refraction corrected. Given that the IS-2 data does not currently operate off-nadir pointing, longitude and latitude corrections were minimal and photon depth correction was approximately 25% (at high precision) shallower than the value recorded in the ATL03 data, in line with the calculations of Parrish et al (2019). A bathymetric profile was manually selected from the corrected photons. Manual data selection yielded a higher signal-to-noise ratio than trialled automated methods and ensured only high

quality depth information was collected. Examples of the refraction corrected photons and selected bathymetry photons are given in Figure 1 (g, h, i). For each IS-2 pass only the high-power beams were utilized. When input into the SDB model, only IS-2 depth photons with a system assigned "Land Confidence" level of 4 were used. These were aggregated into a Sentinel-2 10-m resolution grid (outlined below) and are shown in Figure 1 (d, e f).

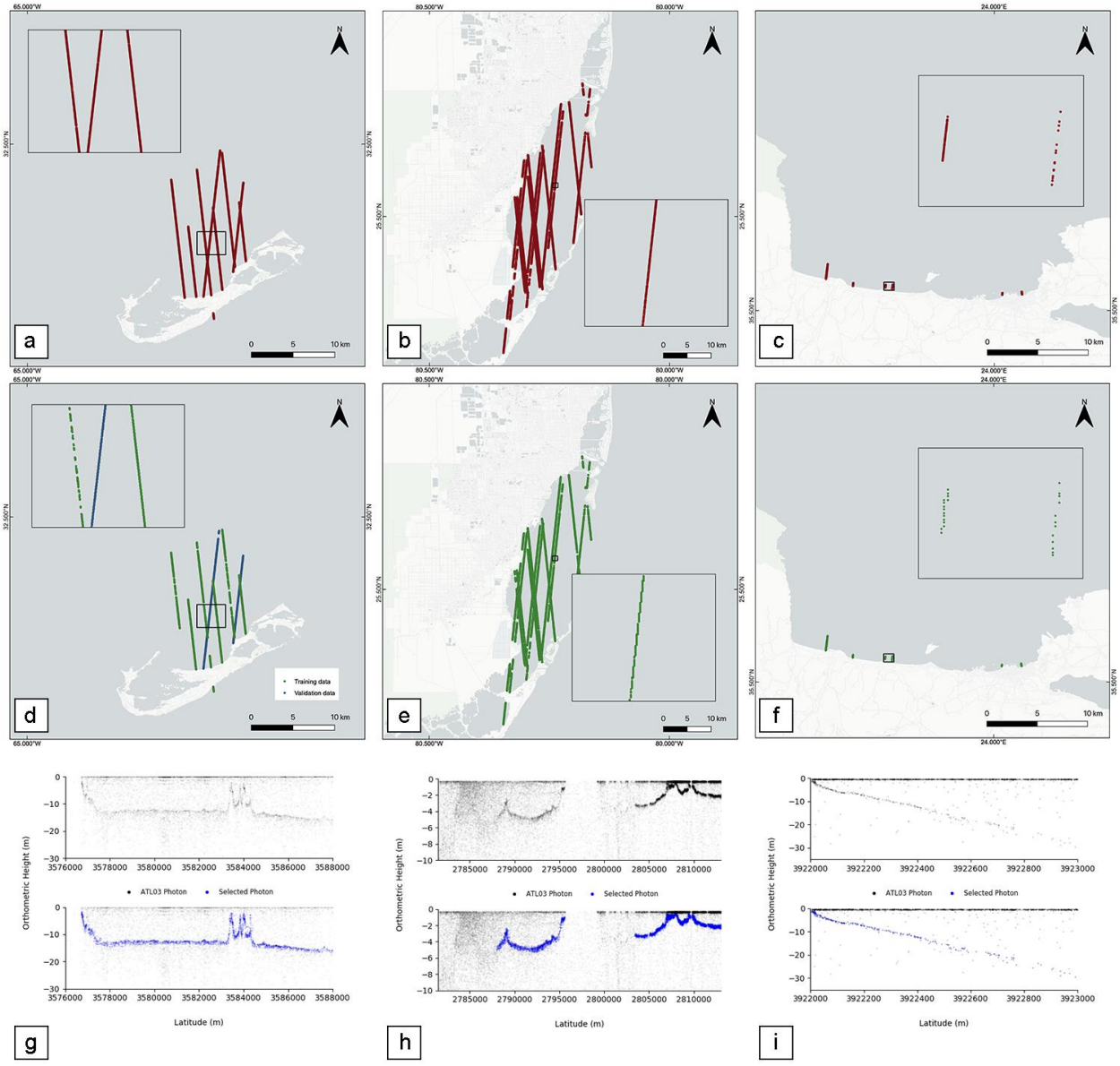

Figure 1: a, b & c) ICESat-2 depth data points for Bermuda, Biscayne Bay and Crete; d, e & f) ICESat-2 depth data points with "Land Confidence" level 4 binned to Sentinel-2 10-m resolution for Bermuda (SDB training (green) and validation (blue)), Biscayne Bay and Crete; g, h & i) ICESat-2 photons and selected bathymetric profile for a single laser transect in Bermuda, Biscayne Bay and Crete.

2.3.2 Sentinel-2 Sattelite Derived Bathymetry (SDB)

To pre-process and synthesize Sentinel-2 data to estimate and scale up the SDB models, we developed a novel cloud-native geoprocessing workflow. This new cloud-based workflow builds on the pre-processing and SDB estimation developed by Traganos et al, (2018a) and Traganos et al, (2018b). Firstly, an evolved cloud mask was developed that combines the GEE-based Sentinel-2 Cloud Probability dataset, the QA60 band, and metadata information. Next, a multi-temporal mosaic was derived using four Sentinel-2 bands; B1-coastal aerosol, B2-blue, B3-green, and B4-red, as these wavelengths are less susceptible to light attenuation. We derived the mosaic using the 20^{th} percentile for each study area data cube to reduce common natural interferences in satellite images over coastal regions, such as sunglint, turbidity, waves, and remaining clouds and haze.

After the initial pre-processing steps, three cloud-based SDB models were derived using the relationship between the multi-temporal satellite data and the IS-2 data: i) a cluster-based linear model merging a k-means unsupervised clustering algorithm (Arthur and Vassilvitskii, 2007) with the algorithm of Lyzenga (1978)—hereafter CBL. This combination ensures that by

splitting the multi-temporal data into numerous classes, each reflectance band adheres to the linear model assumption of homogeneous bottom albedo. This was particularly beneficial in Bermuda and Biscayne Bay which have variable bottom types. Prior to selecting the relevant bands for modeling, we performed preliminary statistical tests with various combinations of Sentinel-2 bands with this method, and acquired the best accuracy with the multilinear regression of B1, B2, B3, and B4. ii) a cluster-based ratio model applying the same k-means clustering algorithm as above, prior to the ratio algorithm of Stumpf et al, (2003)—hereafter CBS. Both CBL and CBS models follow the concept of the cluster-based regression (CBR) algorithm of Geyman and Maloof (2019). Our preliminary statistical tests with various cluster-based ratios identified the B3/B2 ratio as the most accurate model. It is also worth noting that the variable benthic habitats in both Bermuda and Biscayne Bay prompted the use of five clusters in the CBL and CBS SDB models. In contrast, Crete features a mainly homogeneous sandy seabed, averting us from applying clustering prior to the empirical linear and ratio models which we applied and tested here in their original form. iii) a machine learning model based on Support Vector Regression (SVR)—hereafter SVR. We implemented an Epsilon-SVR with the default GEE parameter and a linear kernel to map the first four log-transformed Sentinel-2 bands to a high-dimensional feature space to fit a regression hyperplane. The relationship between IS-2 and Sentinel-2 data, for the best performing model, at each study site is presented in Figure S1.

2.4 Reference Data and Accuracy Assessment

IS-2 data in all three study regions were used to train our three SDB models. We selected only the IS-2 data points with a “Land Confidence” level of 4, within a Sentinel-2 10 m grid (Figure 1). Multiple IS-2 depths within a Sentinel-2 pixel were averaged. We used 80% of the IS-2

observations for training, using three different training/validation approaches for each study site, driven by the availability and quality of reference bathymetric DEM data. A validation sample size of 20% of the IS-2 dataset was used. For the country of Bermuda, we used six IS-2 transects for training (5,173 points) and two IS-2 transects for validation—reduced from 2,510 to 1,293 points to fit the 80/20 ratio. Here, the training and validation data were collected on different days, during different passes, which served as separate independent observations. Initial comparison to a NOAA DEM yielded poor results due to the low temporal and spatial resolution of the DEM (Figure S2 and Figure S3). For Biscayne Bay, IS-2 data was used for training (34,342 points) whereas NOAA bathymetric DEM data was used for validation, using 8,585 (20%) random-stratified points. Lastly, an amalgamation of training with IS-2 data (133 points) and with validation data collected from *in-situ* singlebeam data (85 points) was used in Crete.

For each validation, we calculated the root mean square error (RMSE) and mean absolute error (MAE) as well as the standard deviation of the bathymetry estimation. Residual maps to identify the spatial distribution of the differences between the SDB models and the corresponding NOAA DEMs in Bermuda and Biscayne Bay were also generated (Figure S3 and Figure S4).

3 Results

The CBL method produced the most reliable SDB estimates at all sites with a RMSE of 2.62 m, 0.83 m, and 2.19 m, and MAE of 2 m, 0.65 m, and 2.02 m for Bermuda, Biscayne Bay, and Crete, respectively. Among the three methods, SVR tends to underestimate the range of the depths, although its error values do not differ much from that of the CBL method. The RMSEs of the CBL models are lower or close to 10% of the maximum depth for the Bermuda (26 m) and Crete (22 m) models, but close to 17% for the Biscayne Bay model where the maximum depth of

the modeled area is much lower (5 m). The variance of the models for Bermuda, Biscayne Bay, and Crete were 0.68, 0.79, and 0.83, respectively (Figure 2 j-l). The reference and the modeled depths of Bermuda (Figure 2 j) are in good agreement mostly between the depths of 11-17 m, whereas for the shallower Biscayne Bay (Figure 2 k) it is between 1.2-3 m.

Table 1: Root mean square error, mean average error, and variance of the SDB model vs validation dataset in Bermuda, Biscayne Bay, and Crete

SITE	METHOD	RMSE (M)	MAE (M)	R^2	MAX DEPTH (M)*
BERMUDA	**CBL**	2.62	2.00	0.58	26
	CBS	2.89	2.21	0.50	26
	SVR	2.96	2.00	0.43	26
BISCAYNE BAY	**CBL**	0.83	0.65	0.72	5
	CBS	1.07	0.90	0.30	5
	SVR	0.89	0.73	0.64	5
CRETE	**CBL**	2.19	2.02	0.89	22
	CBS	2.41	2.18	0.85	22
	SVR	3.70	2.52	0.75	22

*based on the IS-2 training datasets

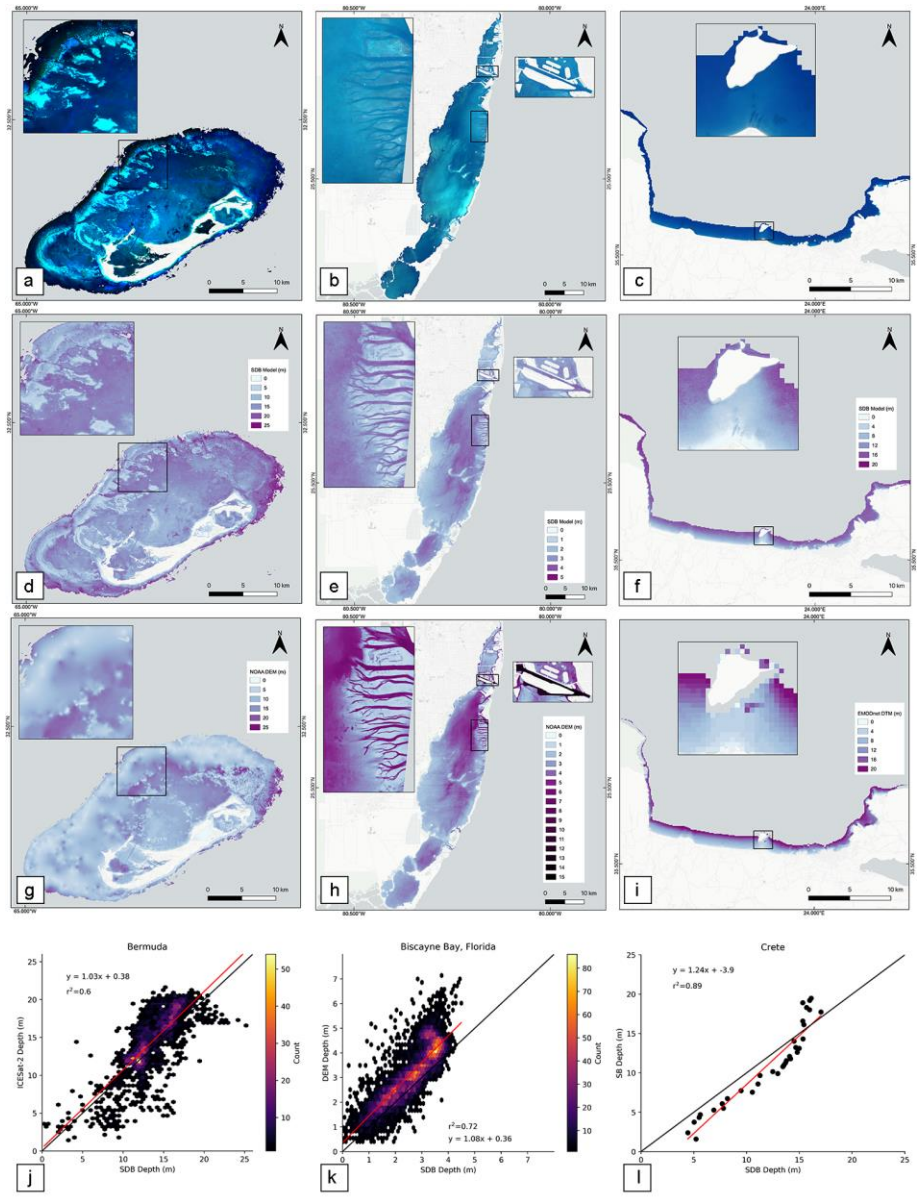

Figure 2: a, b, c) Sentinel-2 RGB synthesis. a) Bermuda: 53 L2A Surface Reflectance tiles, 597 km^2 (March 28, 2017 – April 20, 2020); b) Biscayne Bay: 583 L1C Top-Of-Atmosphere tiles, 689 km^2 (January 1, 2015 – December 31,2019); c) Crete: L1C 403L1C Top-Of-Atmosphere, 61km^2 (January 1, 2015 – December 31,2019). d, e, f) CBL Bathymetry SDB at Bermuda, Biscayne Bay and Crete. g, h, i) NOAA DEM at Bermuda and Biscayne Bay and EMODnet at Crete, j, k, l) SDB-IS2 depth comparison at Bermuda, Biscayne Bay and Crete.

3.1 Comparison with publicly available DEM data

The detailed Bermuda SDB model picks up the bathymetric relief and rugosity of the shallow and coral reef areas in more detail compared to the NOAA DEM product (Figure 2 d and g). The Bermuda NOAA DEM product is a merge of multiple datasets and heavily interpolated in sparsely covered region where navigation is difficult. For this reason, we observe high residuals between the Bermuda SDB and NOAA DEM in the coral reef complexes (Figure 34). Similarly, in shallow water regions, the Bermuda SDB model resolved the detailed relief of the seabed which the NOAA DEM did not (Figure 2 h). With the variance of 0.14, the relationship between SDB and NOAA DEM depths in Bermuda shows a very low agreement (Figure S2) specifically at depths greater than 11 m. The mapped residuals range from -55.96 m to 51.28 m, where negative values occur near patch reef complexes and positive values occur within the spur and groove formations of the coral reef rim

In Biscayne Bay, the SDB model underestimates the depths of the navigation channels compared to the Biscayne Bay NOAA DEM (Figure 2 e and h). More specifically, IS2 could not retrieve the water depth in the deep dredged channels around the Miami Port (Figure 2 h), which reach a depth of 17 m. The mapped residuals range from -14.11 m to 2.86 m (Figure S4). As the IS-2 photons are manually selected, it is noteworthy that photons were able to penetrate the water to the depths of these channels, but did not exhibit an obvious surface for selection and were thus omitted to avoid the use of incorrect depths in the model.

For the Crete study site, however, the SDB models under predict the deeper depths, specifically greater than a depth of 15 m, where the water is optically deep. Here the relationship between IS-

2 reference depths and the log-transformed S-2 reflecance values become non-linearThe reference and the modeled depths of Crete are in good agreement mostly between the depth of 7-15 m. We obtained an available bathymetric map for the Crete study site for qualitative comparison, but not for validation, from EMODNET, with a resolution of ~115 m (Figure 2 i). The EMODnet bathymetry model has a reduced precision compared to the SDB and only consists of integer values for each pixel. Compared to the EMODNET bathymetry map, our Crete SDB model is in much higher spatial resolution (10 m), and features a more gradual change of depths.

4 Discussion and Conclusions

In this study, we have demonstrated the unique fusion of ICESat-2 and Sentinel-2 data for measuring coastal ecosystem structure and shallow water bathymetry, from coastline to country scales. We developed adaptive bathymetry estimation methods derived solely from space-borne observations over coastal waters in Bermuda, Biscayne Bay, and Crete at high-resolution and with low error. The GEE cloud computing platform provides large computational power and a well-integrated system to process hundreds of multi-temporal images in short time, as well as perform analysis with thousands of data points with ease. The high resolution of Sentinel-2 and ICESat-2 data allows us to map benthic variability in detail, improving upon available bathymetry maps, especially within optically shallow water where the reflectance values between different depths are more distinguishable.

We have demonstrated that our approach can yield products that are comparable to, and even improve upon, locally collected existing data. At our study site locations, existing DEM data were composed of multiple methods collected over a large temporal period at varying

resolutions. Therefore, changes in seabed structure due to hydrodynamic processes (such as sediment deposition) and natural catastrophes could have been overlooked. At Biscayne Bay, while our RSME error was small, some uncertainty can be attributed to differences between the high resolution SDB model and lower temporal and spatial resolution NOAA DEM. However, sources of uncertainty are also recognized in the remotely sensed data. At Biscayne Bay, IS-2 was unable to detect the bottom of dredged channels, which may have been caused by sediment (turbidity in active shipping lanes) or the inability of the photons to reliably penetrate to those depths. As the IS-2 bathymetric photons were manually selected, photons at these depths were omitted as they did not not form a coherent reflecting surface. While this limits the introduction of noise into the model it also highlights potential sources of error that are introduced due to user interpretation. This error may also be present in Bermuda and Crete, particularly where IS-2 was used as both training and validation data. Furthermore, a more general source of uncertainty was the effect of tide level in the analysis. By creating Sentinel-2 composite images using the 20% percentile of tens to hundreds of tiles, we collected the darkest reflectance values, which might not coincide with the depth values acquired by the IS-2 platform on a certain acquisition date. The tidal range for our study sites was microtidal (< 1 m) thus the advantages of the approach over the small introduction of error are interpreted to be an acceptable tradeoff.

The SDB models obtained with this approach are capable of contributing to the development of the Blue Economy. Without the requirement for *in situ* data, repeat bathymetric maps can be created for customized time-periods. This flexibility is required for monitoring changes in nearshore topography for the purposes of navigation (Mavraeidopoulos et al, 2017), site assessments, post-disaster mobilization and response (Stronko, 2013), infrastructure

developments (Coughlan et al, 2020), and for bathymetry and benthic cover mapping in regions where field data acquisitions are scarce or prevented by a hazardous environment. Coastal zones will experience a future increase in development and impacts from storm events (Horton et al, 2015) and therefore the need for contemporary and repeat bathymetric observations, particularly for data poor regions, will be critical for ensuring sustainability of coastal resources. This is particularly pertinent for "Big Ocean States" (or "Small Island Nations") which may lack the capacity to carry out bathymetric surveys of their territories (Purkis et al, 2019). A purely space-borne cloud-based method empowers them to conduct their own structural and ecological assessments.

Furthermore, our demonstrated method will allow the development of a global map of coastal submerged ecosystems, which continues to be a critical need of the Blue Economy community. This would be the foundation of global habitat accounting for currently poorly mapped sub-aquatic ecosystems. Indeed, the need of global distribution maps for seagrasses, a blue carbon ecosystem, has been an issue in coastal ecosystem studies, global conservation efforts and national climate change policy agendas (Unsworth et al, 2019). We believe that by scaling up our approach, we will be able to contribute one of the key factors in making a global map of seagrass, and other shallow benthic habitats, possible.

Acknowledgments, Samples, and Data

The authors acknowledge the assistance of Christopher Parrish, Lori Magrider, Amy Neuenschwander and Mike Alonzo for their guidance in correcting bathymetric ICESat-2 photons for the effects of refraction.

This research was funded by NASA Studies with ICESat-2 Program (Grant No. 80NSSC20K0968). Avi Putri Pertiwi and Dimosthenis Traganos acknowledge funding for their efforts from the German Aerospace Center (DLR) through the Global Seagrass Watch project. Dimitris Poursanidis acknowledges terraSolutions marine environment research for the support in bathymetry data collection for the project “Coastal habitat mapping in support of conservation activities for the loggerhead Caretta caretta” funded by MEDPAN.

Datasets are available at: https://doi.org/10.6084/m9.figshare.13017209.v1

References

Albright, A. and Glennie, C., 2020. Nearshore Bathymetry From Fusion of Sentinel-2 and ICESat-2 Observations. *IEEE Geoscience and Remote Sensing Letters*.

Arthur, D. and Vassilvitskii, S., k-means++: The Advantages of Careful Seeding, SODA’07 Proceedings of the eighteenth annual ACM-SIAM symposium on Discrete algorithms, New Orleans, Louisiana, 2007. *URL https://theory. stanford. edu/~ sergei/papers/kMeansPP-soda. pdf*, pp.1027-1035.

Lyons, M., M. Roelfsema, C., V. Kennedy, E., M. Kovacs, E., Borrego-Acevedo, R., Markey, K., Roe, M., M. Yuwono, D., L. Harris, D., R. Phinn, S. and Asner, G.P., 2020. Mapping the world's coral reefs using a global multiscale earth observation framework. *Remote Sensing in Ecology and Conservation*.

Bishop, M.J., Peterson, C.H., Summerson, H.C., Lenihan, H.S. and Grabowski, J.H., 2006. Deposition and long-shore transport of dredge spoils to nourish beaches: impacts on benthic infauna of an ebb-tidal delta. *Journal of Coastal Research*, *22*(3 (223)), pp.530-546.

Caballero, I. and Stumpf, R.P., 2020a. Atmospheric correction for satellite-derived bathymetry in the Caribbean waters: from a single image to multi-temporal approaches using Sentinel-2A/B. *Optics Express*, *28*(8), pp.11742-11766.

Caballero, I. and Stumpf, R.P., 2020b. Towards routine mapping of shallow bathymetry in environments with variable turbidity: contribution of Sentinel-2A/B satellites mission. *Remote Sensing*, *12*(3), p.451.

Caballero, I., Stumpf, R.P. and Meredith, A., 2019. Preliminary assessment of turbidity and chlorophyll impact on bathymetry derived from Sentinel-2A and Sentinel-3A satellites in South Florida. *Remote Sensing*, *11*(6), p.645.

Carey, R.O., Migliaccio, K.W., Li, Y., Schaffer, B., Kiker, G.A. and Brown, M.T., 2011. Land use disturbance indicators and water quality variability in the Biscayne Bay Watershed, Florida. *Ecological Indicators*, *11*(5), pp.1093-1104.

441 Casal, G., Harris, P., Monteys, X., Hedley, J., Cahalane, C. and McCarthy, T., 2020.
442 Understanding satellite-derived bathymetry using Sentinel 2 imagery and spatial prediction
443 models. *GIScience & Remote Sensing*, *57*(3), pp.271-286.
444
445 Casal, G., Hedley, J.D., Monteys, X., Harris, P., Cahalane, C. and McCarthy, T., 2020. Satellite-
446 derived bathymetry in optically complex waters using a model inversion approach and Sentinel-2
447 data. *Estuarine, Coastal and Shelf Science*, p.106814.
448
449 Christianen, M.J., van Belzen, J., Herman, P.M., van Katwijk, M.M., Lamers, L.P., van Leent,
450 P.J. and Bouma, T.J., 2013. Low-canopy seagrass beds still provide important coastal protection
451 services. *PloS one*, *8*(5), p.e62413.
452
453 Coates, K.A., Fourqurean, J.W., Kenworthy, W.J., Logan, A., Manuel, S.A. and Smith, S.R.,
454 2013. Introduction to Bermuda: geology, oceanography and climate. In *Coral reefs of the United*
455 *Kingdom overseas territories* (pp. 115-133). Springer, Dordrecht.
456
457 Coughlan, M., Long, M. and Doherty, P., 2020. Geological and geotechnical constraints in the
458 Irish Sea for offshore renewable energy. *Journal of Maps*, *16*(2), pp.420-431.
459
460 Daly, C.J., Baba, W., Bergsma, E., Almar, R. and Garlan, T., 2020. The New Era of Regional
461 Coastal Bathymetry from Space: A Showcase for West Africa using Sentinel-2 Imagery.
462

de Paiva, J.N.S., Walles, B., Ysebaert, T. and Bouma, T.J., 2018. Understanding the conditionality of ecosystem services: The effect of tidal flat morphology and oyster reef characteristics on sediment stabilization by oyster reefs. *Ecological Engineering*, *112*, pp.89-95.

EMODnet Bathymetry Consortium, 2016. EMODnet Digital Bathymetry (DTM 2016).

Foley, M.M., Halpern, B.S., Micheli, F., Armsby, M.H., Caldwell, M.R., Crain, C.M., Prahler, E., Rohr, N., Sivas, D., Beck, M.W. and Carr, M.H., 2010. Guiding ecological principles for marine spatial planning. *Marine policy*, *34*(5), pp.955-966.

Geyman, E.C. and Maloof, A.C., 2019. A simple method for extracting water depth from multispectral satellite imagery in regions of variable bottom type. *Earth and Space Science*, *6*(3), pp.527-537.

Gorelick, N., Hancher, M., Dixon, M., Ilyushchenko, S., Thau, D. and Moore, R., 2017. Google Earth Engine: Planetary-scale geospatial analysis for everyone. *Remote sensing of Environment*, *202*, pp.18-27.

Harris, D.L., Rovere, A., Casella, E., Power, H., Canavesio, R., Collin, A., Pomeroy, A., Webster, J.M. and Parravicini, V., 2018. Coral reef structural complexity provides important coastal protection from waves under rising sea levels. *Science Advances*, *4*(2), p.eaao4350.

485 Horton, R., Little, C., Gornitz, V., Bader, D. and Oppenheimer, M., 2015. New York City Panel
486 on Climate Change 2015 report chapter 2: Sea level rise and coastal storms. *Annals of the New*
487 *York Academy of Sciences*, *1336*(1), pp.36-44.
488
489 Janowski, L., Trzcinska, K., Tegowski, J., Kruss, A., Rucinska-Zjadacz, M. and Pocwiardowski,
490 P., 2018. Nearshore benthic habitat mapping based on multi-frequency, multibeam echosounder
491 data using a combined object-based approach: A case study from the Rowy site in the southern
492 Baltic sea. *Remote Sensing*, *10*(12), p.1983.
493
494 Kapoor, D.C., 1981. General bathymetric chart of the oceans (GEBCO). *Marine Geodesy*, *5*(1),
495 pp.73-80.
496
497 Kerr, J.M. and Purkis, S., 2018. An algorithm for optically-deriving water depth from
498 multispectral imagery in coral reef landscapes in the absence of ground-truth data. *Remote*
499 *Sensing of Environment*, *210*, pp.307-324.
500
501 Kim, H., Lee, S.B. and Min, K.S., 2017. Shoreline change analysis using airborne LiDAR
502 bathymetry for coastal monitoring. *Journal of Coastal Research*, (79), pp.269-273.
503
504 Lester, S.E., White, C., Mayall, K. and Walter, R.K., 2016. Environmental and economic
505 implications of alternative cruise ship pathways in Bermuda. *Ocean & Coastal*
506 *Management*, *132*, pp.70-79.
507

Li, J., Knapp, D.E., Schill, S.R., Roelfsema, C., Phinn, S., Silman, M., Mascaro, J. and Asner, G.P., 2019. Adaptive bathymetry estimation for shallow coastal waters using Planet Dove satellites. *Remote Sensing of Environment*, *232*, p.111302.

Lirman, D., Deangelo, G., Serafy, J., Hazra, A., Hazra, D.S., Herlan, J., Luo, J., Bellmund, S., Wang, J. and Clausing, R., 2008. Seasonal changes in the abundance and distribution of submerged aquatic vegetation in a highly managed coastal lagoon. *Hydrobiologia*, *596*(1), p.105.

LiVecchi, A., Copping, A., Jenne, D., Gorton, A., Preus, R., Gill, G., Robichaud, R., Green, R., Geerlofs, S., Gore, S. and Hume, D., 2019. Powering the blue economy; exploring opportunities for marine renewable energy in maritime markets. *US Department of Energy, Office of Energy Efficiency and Renewable Energy. Washington, DC*, p.207.

Lyzenga, D.R., 1985. Shallow-water bathymetry using combined lidar and passive multispectral scanner data. *International Journal of Remote Sensing*, *6*(1), pp.115-125.

Ma, Y., Xu, N., Liu, Z., Yang, B., Yang, F., Wang, X.H. and Li, S., 2020. Satellite-derived bathymetry using the ICESat-2 lidar and Sentinel-2 imagery datasets. *Remote Sensing of Environment*, *250*, p.112047.

Marks, K., 2019. The IHO-IOC GEBCO Cook Book.

Mateo-Pérez, V., Corral-Bobadilla, M., Ortega-Fernández, F. and Vergara-González, E.P., 2020. Port Bathymetry Mapping Using Support Vector Machine Technique and Sentinel-2 Satellite Imagery. *Remote Sensing*, *12*(13), p.2069.

Mavraeidopoulos, A.K., Pallikaris, A. and Oikonomou, E., 2017. Satellite derived bathymetry (SDB) and safety of navigation. *The International Hydrographic Review*.

Markus, T., Neumann, T., Martino, A., Abdalati, W., Brunt, K., Csatho, B., Farrell, S., Fricker, H., Gardner, A., Harding, D. and Jasinski, M., 2017. The Ice, Cloud, and land Elevation Satellite-2 (ICESat-2): science requirements, concept, and implementation. *Remote Sensing of Environment*, *190*, pp.260-273.

Narayan, S., Beck, M.W., Reguero, B.G., Losada, I.J., Van Wesenbeeck, B., Pontee, N., Sanchirico, J.N., Ingram, J.C., Lange, G.M. and Burks-Copes, K.A., 2016. The effectiveness, costs and coastal protection benefits of natural and nature-based defences. *PloS one*, *11*(5), p.e0154735.

NOAA. 1998. Biscayne Bay, FL (S200) Bathymetric Digital Elevation Model(30 meter resolution) Derived From Source Hydrographic SurveySoundings Collected by NOAA

Pan, Z., Glennie, C., Legleiter, C. and Overstreet, B., 2015. Estimation of water depths and turbidity from hyperspectral imagery using support vector regression. *IEEE Geoscience and Remote Sensing Letters*, *12*(10), pp.2165-2169.

Parrish, C.E., Magruder, L.A., Neuenschwander, A.L., Forfinski-Sarkozi, N., Alonzo, M. and Jasinski, M., 2019. Validation of ICESat-2 ATLAS bathymetry and analysis of ATLAS's bathymetric mapping performance. *Remote Sensing*, *11*(14), p.1634.

Poursanidis, D., Topouzelis, K. and Chrysoulakis, N., 2018. Mapping coastal marine habitats and delineating the deep limits of the Neptune's seagrass meadows using very high resolution Earth observation data. *International journal of remote sensing*, *39*(23), pp.8670-8687.

Poursanidis, D., Traganos, D., Chrysoulakis, N. and Reinartz, P., 2019. Cubesats allow high spatiotemporal estimates of satellite-derived bathymetry. *Remote Sensing*, *11*(11), p.1299.

Purkis, S.J., Gleason, A.C., Purkis, C.R., Dempsey, A.C., Renaud, P.G., Faisal, M., Saul, S. and Kerr, J.M., 2019. High-resolution habitat and bathymetry maps for 65,000 sq. km of Earth's remotest coral reefs. *Coral Reefs*, *38*(3), pp.467-488.

Ryan, W.B., Carbotte, S.M., Coplan, J.O., O'Hara, S., Melkonian, A., Arko, R., Weissel, R.A., Ferrini, V., Goodwillie, A., Nitsche, F. and Bonczkowski, J., 2009. Global multi-resolution topography synthesis. *Geochemistry, Geophysics, Geosystems*, *10*(3).

Schweiger, C., Koldrack, N., Kaehler, C. and Schuettrumpf, H., 2020. Influence of Nearshore Bathymetry Changes on the Numerical Modelling of Dune Erosion. *Journal of Coastal Research*, *36*(3), pp.545-558.

Spalding, M.D., Ruffo, S., Lacambra, C., Meliane, I., Hale, L.Z., Shepard, C.C. and Beck, M.W., 2014. The role of ecosystems in coastal protection: Adapting to climate change and coastal hazards. *Ocean & Coastal Management*, *90*, pp.50-57.

Stronko, J.M., 2013. *Hurricane Sandy Science Plan—Coastal Topographic and Bathymetric Data to Support Hurricane Impact Assessment and Response* (No. 2013-3099). US Geological Survey.

Stumpf, R.P., Holderied, K. and Sinclair, M., 2003. Determination of water depth with high-resolution satellite imagery over variable bottom types. *Limnology and Oceanography*, *48*(1part2), pp.547-556.

Sutherland, M.G., McLean, S.J., Love, M.R., Carignan, K.S. and Eakins, B.W., 2014. Digital Elevation Models of Bermuda: Data Sources, Processing and Analysis. *Boulder, CO: NOAA National Geophysical Data Center, US Dept. of Commerce*, *7*.

Traganos, D., Poursanidis, D., Aggarwal, B., Chrysoulakis, N. and Reinartz, P., 2018a. Estimating satellite-derived bathymetry (SDB) with the google earth engine and sentinel-2. *Remote Sensing*, *10*(6), p.859.

Traganos, D., Aggarwal, B., Poursanidis, D., Topouzelis, K., Chrysoulakis, N. and Reinartz, P., 2018b. Towards global-scale seagrass mapping and monitoring using Sentinel-2 on Google Earth Engine: The case study of the aegean and ionian seas. *Remote Sensing*, *10*(8), p.1227.

Unsworth, R.K., McKenzie, L.J., Collier, C.J., Cullen-Unsworth, L.C., Duarte, C.M., Eklöf, J.S., Jarvis, J.C., Jones, B.L. and Nordlund, L.M., 2019. Global challenges for seagrass conservation. *Ambio*, *48*(8), pp.801-815.

Wessel, B., Huber, M., Wohlfart, C., Marschalk, U., Kosmann, D. and Roth, A., 2018. Accuracy assessment of the global TanDEM-X Digital Elevation Model with GPS data. *ISPRS Journal of Photogrammetry and Remote Sensing*, *139*, pp.171-182.

Wölfl, A.C., Snaith, H., Amirebrahimi, S., Devey, C.W., Dorschel, B., Ferrini, V., Huvenne, V.A., Jakobsson, M., Jencks, J., Johnston, G. and Lamarche, G., 2019. Seafloor Mapping–the challenge of a truly global ocean bathymetry. *Frontiers in Marine Science*, *6*, p.283.

Zhang, Z., Huang, H., Liu, Y., Bi, H. and Yan, L., 2020. Numerical study of hydrodynamic conditions and sedimentary environments of the suspended kelp aquaculture area in Heini Bay. *Estuarine, Coastal and Shelf Science*, *232*, p.106492.